

LETTER TO THE EDITOR

Shape-resonance-induced long-range molecular Rydberg states

Edward L Hamilton¹, Chris H Greene¹ and H R Sadeghpour²

¹ Department of Physics and JILA, University of Colorado, Boulder, CO 80309-0440, USA

² ITAMP, Harvard-Smithsonian Center for Astrophysics, 60 Garden Street, Cambridge, MA 02138, USA


Received 22 April 2002

Published 8 May 2002

Online at stacks.iop.org/JPhysB/35/L199

Abstract

When an excited atomic electron interacts with a neutral perturbing atom or molecule that possesses a shape resonance, it generates a characteristic class of Born–Oppenheimer potential curves that rise with internuclear distance. We document this effect, and predict the existence of a diverse class of stable, strongly bound atom–atom and atom–molecule states that result from this phenomenon. For the specific case in which Rb is the perturbing atom, we show that such states should be observable in the spectroscopy of an ultracold gas or condensate.

 This article features online multimedia enhancements

When an atom in a low-lying excited state or a Rydberg state is brought near a ground state atom or molecule, much of the interaction derives from simple electron scattering off the ground state species. This picture was developed in a classic paper by Fermi [1] to describe pressure shifts of atomic Rydberg spectral lines. In a high Rydberg state, the electron kinetic energy is so low that the electron–perturber scattering is primarily s-wave, and in that case the main physics is carried by the s-wave scattering length. A recent study [2] showed that, in an ultracold gas, the negative ³S-wave scattering length can produce a new type of ultralong-range molecule with unusual properties. The purpose of this letter is to predict the existence of a new and very different class of long-range molecular states that arise when the electron–perturber scattering exhibits a shape resonance. Electron–atom or electron–molecule shape resonances have been studied extensively in their own right, but their manifestation as features in a Born–Oppenheimer molecular potential curve or surface has apparently not been elucidated. Among the properties that we predict are: (i) much stronger binding energies than were predicted for other predicted classes of long-range Rydberg states; (ii) in some cases, the existence of large permanent electric dipole moments.

Creation, storage and manipulation of cold dilute atomic gases by laser and magnetic cooling have spawned novel and high-precision spectroscopic analyses of atomic and molecular

transitions (see [3], and others). The near-threshold photoionization of cold atoms, for example, results in the subsequent evolution of the entire sample into a cold neutral plasma, by a process that may mirror the Mott insulator–conductor phase transition [4, 5]. For excitation to a Rydberg state just below threshold, neutral atoms may be placed into a frozen gas state which exhibits long-range many-body coupling effects [6]. Very recently, the formation of a large number of Rydberg atoms in an expanding ultracold neutral plasma has been reported [7]. In particular, dipole–dipole interactions have been proposed as a candidate for quantum logic operations [8]. Other proposals for studying and manipulating cold Rydberg matter include the use of a ponderomotive optical lattice as a controlled trapping environment [9] and the extension of atom-to-ion charge mobility studies to excited atomic states where charge hopping may be greatly enhanced [10]. Due to the low thermal energy and large internuclear spacing of such systems, they should similarly provide an ideal laboratory for the investigation of delicate long-range interactions between Rydberg atoms and neutral ground state atoms or molecules.

The outer electron of a Rydberg atom is distributed over a region that extends far from the ionic core. At large radii the Coulomb potential is weak, and varies slowly as a function of position; consequently, the valence electron has low momentum and may be viewed as occupying a ‘quasi-free’ state. This allows the interaction between a nearby ground state particle (the ‘perturber’) and the Rydberg atom to be described in terms of isolated scattering events between the electron and perturber and between the electron and the ionic core. In effect, the three-body problem (electron, ion, and perturber) is treated as a combination of two separate two-body interactions. Spin–orbit effects are neglected in this paper.

As noted above, this model has already been used to predict the existence of two classes of ultralong-range (i.e. of size 10^2 – 10^4 au) Rydberg molecular bound states in an ultracold Rb gas; these molecules consist of one excited and one ground state atom [2]. In addition to being much larger than any diatomic bound state yet observed, these molecules are expected to have permanent electric dipole moments in the kilodebye (kD) range, and lifetimes on the order of tens or hundreds of microseconds. The Born–Oppenheimer potential curves of these states are oscillatory, with many local minima, each supporting multiple vibrational levels. The second class, the perturbed hydrogenic states [11, 12], also have an unusual valence electron probability distribution resembling a trilobite fossil, which can be viewed as a semiclassical electron interference pattern [13]. Both classes of molecular states, however, are bound only weakly, by just a small fraction of the spacing between adjacent n -manifolds. For $n = 30$, for example, the minimum of the first type of state is approximately 100 MHz, whereas the minimum of the second type is roughly 10 GHz, compared to the 250 GHz separation between the $n = 30$ and 29 manifolds.

Ordinarily, the scattering of a low-energy electron (such as a Rydberg electron far from the core) can be well approximated by including only s-wave scattering. This is a familiar consequence of the Wigner threshold law. When the angular momentum of the scattered electron relative to the perturbing particle is greater than zero, however, the short-range potential may support quasi-bound negative ion states, e.g. shape resonances. Since the scattering parameters vary rapidly as a function of energy in the vicinity of a shape resonance, such resonance channels can result in the formation of molecular bound states.

The quasi-free electron picture was first developed by Fermi [1] to explain the spectral line shifts of Rydberg atoms in a buffer gas. Fermi’s original theory introduced a delta-function interaction proportional to the scattering length, the so-called Fermi pseudopotential. This well-known result corresponds to the scattering length approximation [14], and models low-energy (s-wave-dominated) scattering behaviour with reasonable accuracy. Alternatively, a more general zero-range pseudopotential form appropriate to partial waves beyond $l = 0$ can be formulated using a Green’s-function technique that treats the perturber as an additional

boundary condition on the atomic solution [15]. This approach has been applied fruitfully to the study of electron transfer effects in atomic collisions [16], particularly those in which the collision is assisted by a laser field that excites one of the atoms into a Rydberg state [17, 18]. A second, and fully equivalent, method applies the zero-range potential as an additional term in the molecular Hamiltonian, consisting of a sum of separable projections for each l -channel onto angular momentum eigenstates [19].

Our treatment of this problem follows a method developed by Omont [20], based on approximating the zero-range pseudopotential with an l -expansion of the R -matrix. For the present results, we shall be content to examine only systems for which the scattering is dominated by the s- and p-wave partial waves, although the same approach should also apply to perturbers with d-wave or f-wave shape resonances (such as N_2 or SF_6 .) We choose to study the ^{87}Rb Rydberg atom, whose large ionic core destroys the orbital angular momentum degeneracy and whose heavy mass ensures the existence of many closely spaced vibrational levels. Rubidium, of course, is a favourite atom utilized in the study of ultracold atomic gases. We shall further assume that experimental ability exists to prepare a Rydberg state containing high-angular-momentum components, either by a multiphoton process or by the imposition of a weak electric field that breaks the dipole selection rule.

The Fermi pseudopotential, appropriate for s-wave scattering, is given by

$$V_s(\vec{r}, \vec{R}) = 2\pi A_T [k(R)] \delta(\vec{r} - \vec{R}) \quad (1)$$

where \vec{r} is the position of the electron, \vec{R} is the position of the perturber, both from the ionic core, $k(R)$ is the valence electron wavenumber, and we define the triplet scattering length for electron-perturber collisions as $A_T = -\tan \delta_0^T / k$. The energy variation of the triplet s-wave phase shift δ_0^T , comes from its implicit dependence on R , according to $\frac{1}{2}k^2(R) = -\frac{1}{2n^2} + \frac{1}{R}$, for a Rydberg electron with principal quantum number n . Following Omont, the matrix element associated with p-wave electron-perturber scattering can be written as

$$\langle \Psi_1 | V_p | \Psi_2 \rangle = -\frac{6\pi \tan \delta_1^T}{k^3(R)} \vec{\nabla} \Psi_1(\vec{R}) \cdot \vec{\nabla}' \Psi_2(\vec{R}) \quad (2)$$

where δ_1^T is now the triplet p-wave scattering phase shift. We adopt the *ab initio* calculations of Bahrim *et al* [21–23] for the s- and p-wave triplet e^- -Rb(5s) scattering phase shifts.

In order to generate a bound state, the perturbation should ideally result in a negative energy shift, though bound states might in some cases result from repulsive scattering lengths. For s-wave scattering, a negative shift translates into a negative scattering length; for p-wave scattering, the tangent of the phase shift must be positive. Qualitatively, these pseudopotentials may be viewed as selecting a linear combination of atomic states that maximizes either the value of the wavefunction (s-wave) or of its derivative (p-wave) at the position of the perturber. Note that for the p-wave correction, the derivative acts in all three spatial directions, giving rise to two possible sets of states: those that maximize the gradient parallel to the internuclear axis, and those that maximize the gradient perpendicular to it. The former have a nodal plane perpendicular to the internuclear axis, and thus a Σ molecular symmetry ($m = 0$), and the latter place the nodal plane along the axis, and hence have a Π molecular symmetry ($m = 1$).

At the position of a resonance, the tangent of the phase shift diverges, resulting in an unphysical form of the interaction potential. In practice, however, the energy eigenstate is bounded by manifolds corresponding to $n + 1$ and $n - 1$, and is subject to level repulsion by states of identical symmetry attached to the adjacent manifolds. This permits a diagonalization even at energies close to the resonance energy, circumventing the need to resort to explicit renormalization of the potential. The number of manifolds retained above and below the n -value of interest can be varied to test the eigenvalue stability.

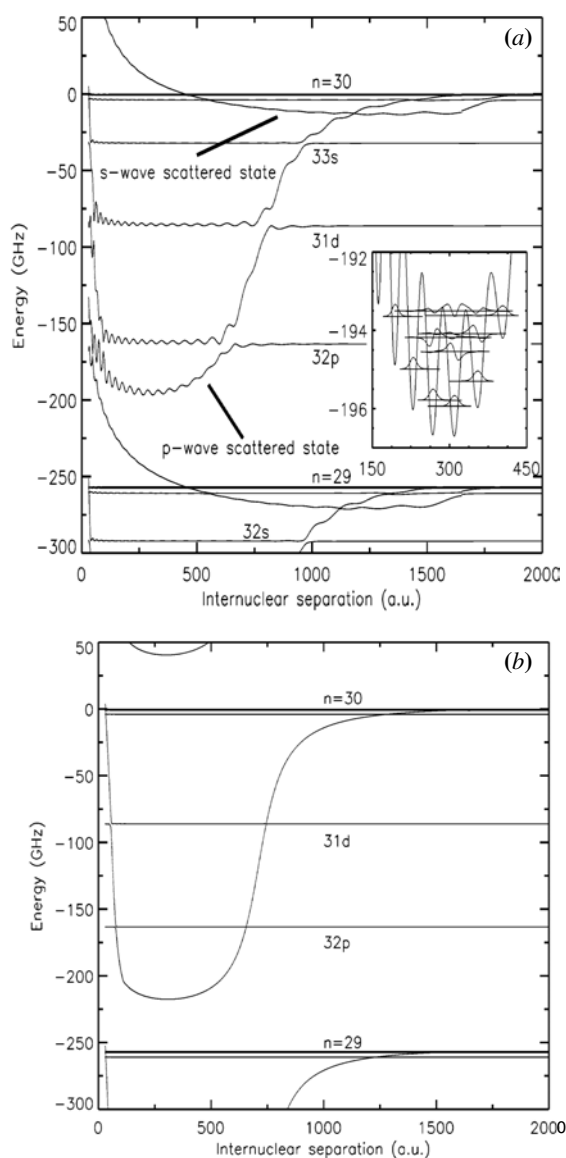


Figure 1. (a) ${}^3\Sigma$ Born–Oppenheimer potential curves for states arising from both s-wave and p-wave scattering. Several of the lowest vibrational levels, along with their associated wavefunctions, are shown in the inset. The zero of the energy axis is taken to lie at the position of the $n = 30$ manifold. (b) ${}^3\Pi$ Born–Oppenheimer potential curve arising from p-wave scattering.

The Born–Oppenheimer potential curves (both s- and p-waves) associated with the Σ molecular symmetry are shown in figure 1(a), and the curve for the Π symmetry state (possible for p-wave only) is shown in figure 1(b). The associated s- and p-wave phase shifts, as functions of position, are shown in figure 2. Recall that the phase shifts at the perturber R are implicit functions of R as a result of the change in the local kinetic energy of the scattered electron. The most prominent qualitative features of the potentials are directly controlled by the energy dependence of the phase shift. For example, the point at which the Σ s-wave

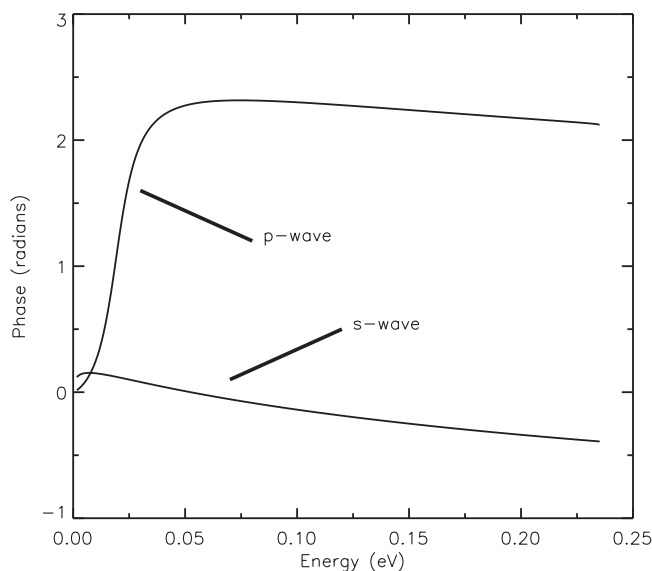


Figure 2. Phase shifts for low-energy s- and p-wave scattering from ^{87}Rb as a function of energy [23]. The Ramsauer–Townsend zero in the s-wave curve at $E = 0.05$ eV corresponds to the point at $R = 450$ where the s-wave potential crosses through the $n = 30$ manifold. The resonance in the p-wave phase shift between 0.02 and 0.04 eV controls the rapid rise of the p-wave potential in the range between $R = 500$ and 1000 au.

potential passes through zero corresponds to the Ramsauer–Townsend zero in the e^- –Rb(5s) phase shift at 0.042 eV (around $R = 450$ au) [2]. For a more detailed discussion of how the small oscillatory minima superimposed on the potentials can arise, see [13].

For the present context, the most notable characteristic of the p-wave potentials is their broad and comparatively deep minimum. As R decreases through the vicinity of the shape resonance around $R = 700$, the associated p-wave potentials detach from the $n = 30$ manifold, pass through a point where the slope of the potential becomes large, and run close to the $n = 29$ manifold for smaller R . In essence, a rise by π in the scattering phase shift due to the p-wave resonance results in a promotion of the associated molecular curve to the next lower manifold. We emphasize that this effect is quite general; it will occur between any two adjacent n -manifolds, for any partial-wave electron–perturber scattering channel that contains a shape resonance. This behaviour should consistently define the existence of a global minimum in the potential curve, and thus a set of bound vibrational levels. In the inset of figure 1(a) we show the first ten vibrational levels for the p-wave scattered Σ state.

Both sets of potential curves exhibit multiple avoided crossings, both with the hydrogenic energy levels, and (in the case of identical molecular symmetry) with each other. Depending on the Landau–Zener parameters for each crossing, sufficiently high vibrational levels may dissociate on a timescale shorter than the natural lifetime of the Rydberg state. Even for states lower in energy than the crossing energy, the possibility of tunnelling cannot be excluded; this is of particular concern for the crossing between s- and p-wave $^3\Sigma$ states, which occurs close to the s-wave minimum and could potentially destabilize even the lowest vibrational level. Based on this and other anticipated decay mechanisms, including a significant contribution from black-body radiation, we predict that the lifetime of such states should scale as n^2 [24] and be of the order of $50 \mu\text{s}$ for $n = 30$. This is longer than the vibrational period of low-

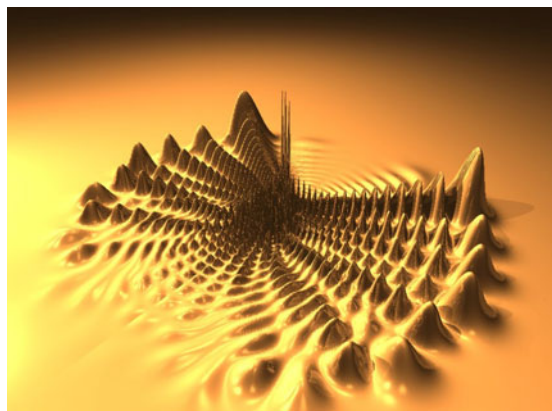


Figure 3. A surface plot of the Rydberg electron probability density in cylindrical coordinates for the $n = 30$ $^3\Sigma$ p-wave scattered ('butterfly') state. The perturber is located at the position of the lowest minimum in the potential energy curve (at $R = 308$ au), and corresponds to the largest peaks in electron density along the axis of symmetry.

lying levels, suggesting the possibility of resolving vibrational substructure in the absorption spectrum.

Figure 3 contains a wavefunction of the Σ p-wave scattered molecular state in the vicinity of the minimum of the potential curve. Rather than being distributed over the entire classically allowed region, the electron density is confined to an envelope with the approximate shape of a butterfly. The nodal pattern features two large 'wings' of electron density extending to the usual spatial boundary of the atomic Rydberg state, but along the internuclear axis the density accumulates near the position of the perturber.

Like the trilobite states controlled by pure s-wave scattering [2], the p-wave 'butterfly' states develop large electric dipole moments, despite the fact that the electron density vanishes at the perturber. The behaviour of the dipole moment at the equilibrium separation with n scales roughly linearly with n , and its value for the $n = 30$ states is approximately 1.05 kD, rising to 3.91 kD for $n = 70$. The Π symmetry states have similarly large dipole moments, but negative, with a value of -1.53 kD at $n = 30$. Such large permanent dipole moments can be manipulated by external electromagnetic fields or by dipole–dipole interactions.

Previous studies have confirmed the utility of the zero-range pseudopotential method in modelling a short-range physical potential [12, 19]. To verify the accuracy of the extension of this technique to p-wave scattering, we performed a full diagonalization on a two-dimensional spline basis set using a nonlocal model pseudopotential with free parameters that could be varied to reproduce the observed phase shifts. (See [25] for a recent example of the application of this method.) As a further test, we also implemented the zero-range potential approximation using a Green's-function technique, as presented in [17]. A comparison of these three methods is shown in figure 4. In each calculation, the overall shape of the p-wave bound state confirms the validity of the extended Fermi model, with quantitative agreement within a few percent. Note that for the sake of this comparison, the core quantum defects have been set to zero (i.e., an H + Rb system), allowing us to use the exact analytic Coulomb Green's function.

These conclusions can be extended to molecular perturbers, through a generalized version of the same zero-range potential [17]. The simplest such system, a diatomic molecular perturber, introduces a second axis of symmetry into the problem, defining the orientation of the molecule, with the result that states of differing molecular symmetry (i.e., projection

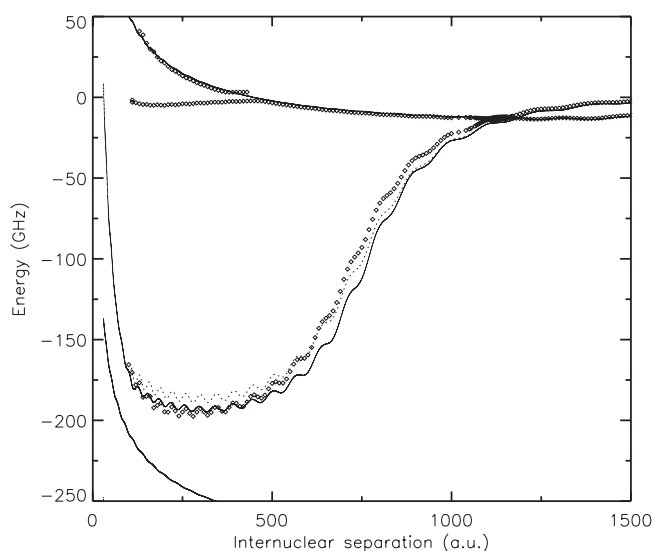


Figure 4. Comparison of the Fermi-style pseudopotential perturbative calculation with two alternative methods of calculating the internuclear potential. Solid: Fermi (as for figure 1); dotted: Green's function; points: diagonalization of a fitted finite-range pseudopotential.

of the electronic angular momentum onto the ion–perturber axis) can become coupled. Note, however, that if the perturber has a permanent dipole moment, the longer-range e –dipole interaction controls the scattering physics, invalidating the assumptions of the zero-range approximation. The large number of shape resonances known in electron–molecule scattering (N_2 , SF_6 , BF_3 , CO_2 , for instance) suggests that this class of Born–Oppenheimer potential curves should be observable in many different contexts, ranging from the conventional quantum chemistry of valence states to the Rydberg states of an ultracold gas.

This work was supported by grants from the National Science Foundation. We wish to thank C Bahrim, U Thumm and I I Fabrikant for providing numerical data for the phase shift parameters, as well as B Granger for insightful discussions and E Eyler and P Gould for providing helpful comments and access to experimental data.

References

- [1] Fermi E 1934 *Nuovo Cimento* **11** 157
- [2] Greene C H, Dickinson A S and Sadeghpour H R 2000 *Phys. Rev. Lett.* **85** 2458
- [3] Weiner J *et al* 1999 *Rev. Mod. Phys.* **71** 1 and references therein
- [4] Kulin S, Killian T C, Bergeson S D and Rolston S L 2000 *Phys. Rev. Lett.* **85** 318
- [5] Robinson M P, Tolra B L, Noel M W, Gallagher T F and Pillet P 2000 *Phys. Rev. Lett.* **85** 4466
- [6] Anderson W R, Veale J R and Gallagher T F 1998 *Phys. Rev. Lett.* **80** 249
- [7] Killian T C *et al* 2001 *Phys. Rev. Lett.* **86** 3759
- [8] Lukin M *et al* 2001 *Phys. Rev. Lett.* **87** 037901
- [9] Dutta S K, Feldbaum D, Walz-Flannigan A, Guest J R and Raitel G 2001 *Phys. Rev. Lett.* **86** 3993
- [10] Cote R 2000 *Phys. Rev. Lett.* **85** 5316
- [11] Du N Y and Greene C H 1987 *Phys. Rev. A* **36** 971
- [12] Du N Y and Greene C H 1989 *J. Chem. Phys.* **90** 6347
- [13] Granger B E, Hamilton E L and Greene C H 2001 *Phys. Rev. A* **64** 2508

-
- [14] Beigman I L 1995 *Phys. Rep.* **250** 95
 - [15] Demkov Y N and Ostrovskii V N 1988 *Zero-Range Potentials and their Applications in Atomic Physics* (New York: Plenum)
 - [16] Ivanov G K 1973 *Opt. Spectrosc.* **37** 361
 - [17] Dubov V S and Rabitz H 1996 *J. Chem. Phys.* **104** 551
 - [18] Dubov V S 1992 *J. Chem. Phys.* **97** 7342
 - [19] de Prunele E 1987 *Phys. Rev. A* **35** 496
 - [20] Omont A 1977 *J. Physique* **38** 1343
 - [21] Bahrim C, Thumm U and Fabrikant I I 2001 *J. Phys. B: At. Mol. Opt. Phys.* **34** L195
 - [22] Bahrim C, Thumm U and Fabrikant I I 2001 *Phys. Rev. A* **63** 042710
 - [23] Bahrim C and Thumm U 2000 *Phys. Rev. A* **61** 022722
 - [24] Cooke W E and Gallagher T F 1980 *Phys. Rev. A* **21** 588
 - [25] Dhrebtukov D B and Fabrikant I I 1995 *Phys. Rev. A* **51** 4675